

# 17 THz Continuous-Wave Optical Modulator

J. J. Weber, J. T. Green, and D. D. Yavuz

*Department of Physics, 1150 University Avenue,  
University of Wisconsin at Madison, Madison, WI, 53706*

(Dated: September 7, 2011)

## Abstract

We use coherently rotating hydrogen molecules and demonstrate a continuous-wave (CW) optical modulator at a frequency of 17.6 THz that can modulate any laser within the optical region of the spectrum. The molecules are prepared in a coherent state by using two intense laser beams spaced by the Raman transition frequency inside a high finesse cavity.

PACS numbers: 42.65.Dr, 42.65.Re, 42.50.Gy

Optical modulators are versatile tools that have found uses in many different scientific disciplines [1]. Modulators typically utilize nonlinear optical processes in crystals, such as electro-optic and acousto-optic effects, and have recently achieved modulation rates approaching 100 gigahertz (GHz) [2]. In this letter, we report an experiment that extends these ideas to much higher modulation frequencies using coherently rotating hydrogen molecules. We describe a continuous-wave (CW) optical modulator at a frequency of 17.6 terahertz (THz) that can modulate any beam within the wavelength range of 120 nm to 10  $\mu\text{m}$  with a single-pass efficiency roughly varying between  $10^{-4}$  and  $10^{-8}$ . In addition to these broadband capabilities, the modulation efficiency of our device is independent of the incident optical power, and therefore our modulator is capable of modulating arbitrarily weak signals.

The effect of an optical modulator on a laser beam can be understood either in the time or in the frequency domain. From a time domain viewpoint, either the intensity or the frequency of the laser beam varies with time, an effect commonly referred to as amplitude modulation (AM) or frequency modulation (FM). In either case, the equivalent effect in the frequency domain is that laser beams at new frequencies separated by the modulation rate are produced. For example, a monochromatic beam at frequency  $\nu_0$  (typically referred to as the carrier) would produce new beams (typically referred to as sidebands) at frequencies  $\nu_0 - \nu_m$  and  $\nu_0 + \nu_m$ , where  $\nu_m$  is the modulation rate. In our experiment,  $\nu_m = 17.6$  THz, so the wavelengths of the sidebands are substantially different from the carrier wavelength. For instance, a carrier at a wavelength of 785 nm produces frequency up-shifted and down-shifted sidebands at wavelengths of 750 nm and 823 nm, respectively.

Before proceeding with a detailed description of our experiment, we would like to discuss possible future applications of such a high-frequency CW modulator. i) As we will discuss below, in the near future we will likely be able to increase the efficiency of our device. With improved efficiency, multiple-modulation orders with frequencies  $\nu_0 + q\nu_m$ , where  $q$  is an integer, may be produced [3, 4]. Together, these multiple sidebands form a broad CW spectrum in which each spectral component has a narrow linewidth. With such a spectrum, one can synthesize arbitrary optical waveforms with unprecedented resolution. ii) The absolute frequency of our modulator may be precisely set by locking the driving lasers to an external optical frequency reference (for example to one of the teeth of a frequency-comb) [5–7]. As a result, if a frequency-stabilized carrier is used, the generated sideband frequencies will also be known to very high precision. This will, for example, allow the construction

of optical clocks in different regions of the spectrum or the generation of a broad absolute frequency reference with components covering much of the optical region. iii) As we discuss below, CW optical modulators can also be used to broaden the spectrum of a frequency-comb Ti:sapphire laser oscillator [8, 9]. This will extend the capabilities of such frequency-combs to previously inaccessible spectral regions, which would lead to wide-ranging applications in fields such as precision spectroscopy and coherent control [5, 10–12].

We next cite important prior work that has led to our experiment. Pulsed modulators based on coherently vibrating or rotating molecules, termed molecular modulators, have been constructed with femtosecond and nanosecond lasers [13, 14]. In their pioneering work, Harris and colleagues used an adiabatic Raman excitation technique to produce a broadband spectrum covering much of the optical region [15–17]. This technique has been continually improved over the last decade, and many exciting results have been reported. Of particular importance, using phase and amplitude control over a subset of the broad spectrum, researchers have synthesized single cycle pulses and arbitrary optical waveforms [18–20]. Despite these exciting developments, pulsed molecular modulators have important limitations and have not yet made a significant impact on other scientific disciplines. Their duty cycle is very low, less than 1 part in  $10^7$ , which severely restricts data rates. Furthermore, each sideband has a minimum linewidth, typically about 100 MHz, determined by the duration of the pulse. As a result, pulsed molecular modulators are not suitable for the applications discussed above. Of particular importance is their incompatibility with frequency-comb Ti:sapphire laser oscillators.

To extend the molecular modulation technique to the CW domain [21], we extend the pioneering experiments of Carlsten and colleagues to the high-coherence, low-pressure regime [22–24]. A summary of our experiment and the relevant energy level diagram are shown in Figs. 1(a) and 1(b). We prepare the molecules to a highly coherent state inside a high finesse cavity with two intense laser fields, the pump and the Stokes, at wavelengths of  $1.064\ \mu\text{m}$  and  $1.134\ \mu\text{m}$ , respectively. We utilize the  $|\nu = 0, J = 1\rangle \rightarrow |\nu = 0, J = 3\rangle$  rotational Raman transition in  $\text{H}_2$ , which has a transition frequency of 17.6 THz. With the molecules prepared in a coherent state, a third, weaker laser beam at a wavelength of 785 nm passes through the system and is modulated to produce frequency up-shifted and down-shifted sidebands at wavelengths of 750 nm and 823 nm, respectively. It is important to note that the mirrors of the cavity do not have a high reflectivity at 785 nm, and thus the modulation is produced

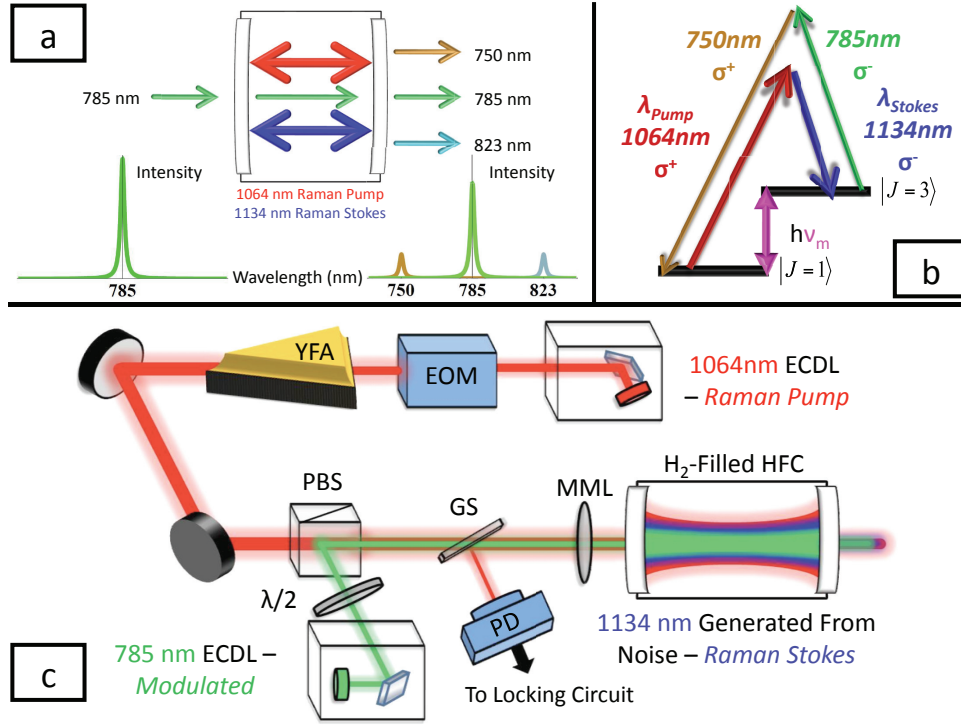


FIG. 1: a) Summary of our experiment. We drive  $\text{H}_2$  molecules to a coherent rotational state using two intense beams, the pump and the Stokes, inside a high finesse cavity. A third laser beam at a wavelength of 785 nm passes through the system and is modulated by the coherently rotating molecules through four-wave mixing. b) Relevant energy level diagram. The  $\sigma^-$  polarization of the carrier produces the frequency up-shifted sideband at a wavelength of 750 nm. Similarly, the  $\sigma^+$  polarization would generate an 823 nm beam (not shown to reduce clutter). c) The simplified schematic of our experiment. ECDL: external cavity diode laser, EOM: electro-optic modulator, YFA: ytterbium fiber amplifier, PBS: polarizing beam splitter, GS: glass slide, PD: photo-diode, MML: mode-matching lens. HFC: high-finesse cavity.

in a single pass through the system. Figure 1(c) shows a simplified experimental schematic. The high-finesse cavity is formed with two dielectric mirrors with high reflectivity at the pump and at the Stokes wavelengths. The cavity is placed inside a vacuum chamber filled with molecular  $\text{H}_2$ .

The pump laser system consists of a custom-built external cavity diode laser (ECDL) whose output is amplified with a CW ytterbium fiber amplifier. We use the Pound-Drever-Hall technique to lock the laser to one of the longitudinal modes of the cavity. Further tech-

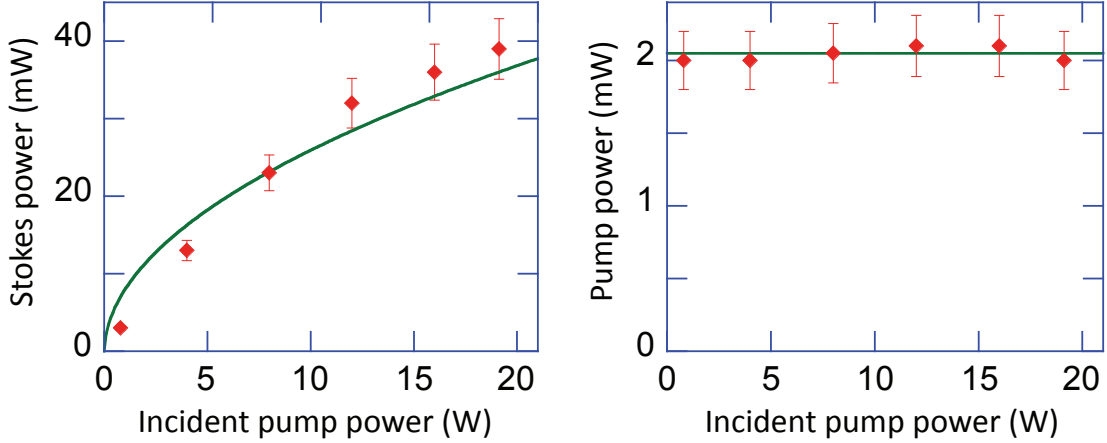


FIG. 2: The transmitted pump and Stokes powers through the output mirror as a function of the incident pump power at a gas pressure of 0.33 atm. The solid lines are fits to the data based on the Raman laser model developed in Ref. [23]. See text for details.

nical details on our experimental set-up can be found in our previous publications [25, 26]. To increase the efficiency of the desired rotational Raman coupling, we circularly polarize the pump beam right before the cavity. When we lock the pump laser to the cavity, we observe CW Raman lasing of the Stokes beam with opposite circular polarization. Figure 2 shows the transmitted pump and Stokes powers through the cavity as the incident pump power is varied. The  $\text{H}_2$  gas pressure in the cavity is 0.33 atm. At the highest incident power, we observe 2 mW of pump and 39 mW of Stokes power transmitted through the output mirror. The solid lines are fits to the data based on the Raman laser model developed by Carlsten and colleagues [23]. The best fit gives  $R_p = 0.9998$  and  $R_s = 0.9992$  for the reflectivities of the mirrors at the pump and the Stokes wavelengths,  $T_p = 80$  parts per million (ppm) and  $T_s = 65$  ppm for the mirror transmissivities at the two wavelengths, and  $\alpha = 4.4 \times 10^{-9}$  cm/W for the plane-wave Raman gain coefficient. We have investigated Raman lasing at pressures ranging from 0.05 to 1.5 atm, and, consistent with the model, we have observed that an increase in pressure is accompanied by a reduction in the transmitted pump and Stokes powers. For example, at a pressure of 0.08 atm, the highest transmitted pump and Stokes powers are 11 mW and 69 mW, whereas at 1.5 atm, these quantities are 1.2 mW and 18 mW, respectively.

We next discuss modulating the carrier beam with the molecular coherence that is established by the intense intracavity fields of the pump and Stokes beams. To generate the carrier beam, we use a separate 785 nm ECDL whose output is amplified by a semiconductor tapered amplifier. The optical power in the carrier before the cavity is about 100 mW. The motivation for amplifying the carrier is to increase the optical power of the generated sidebands to more easily detectable levels. The 785 nm beam is focused to a Gaussian radius of 210  $\mu\text{m}$  at the center of the cavity. For comparison, the cavity mode radii of the pump and the Stokes beams are 405  $\mu\text{m}$  and 418  $\mu\text{m}$ , respectively. After the cavity, we detect the modulation by coupling the 785 nm beam to an optical spectrum analyzer. Due to angular momentum selection rules, if the carrier has the same (opposite) circular polarization as the pump, the frequency down-shifted (up-shifted) sideband is produced. In our experiment, because the carrier beam is combined with the pump beam using polarization-selective optics, we do not have independent control of the carrier beam polarization. The carrier is elliptically polarized, and we produce both up-shifted and down-shifted sidebands at wavelengths of 750 nm and 823 nm with a power ratio of  $P_{750}/P_{823} \approx 3$ .

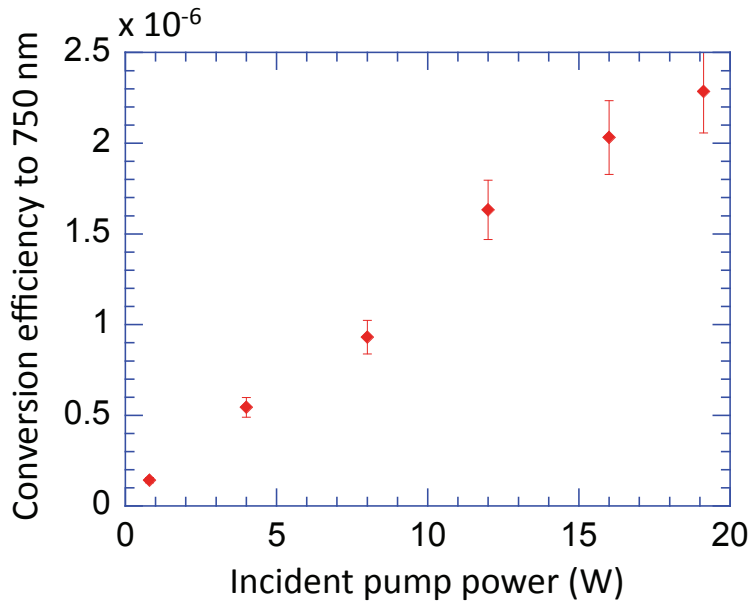


FIG. 3: The conversion efficiency from the carrier to the 750 nm sideband as the incident pump power is varied at a constant  $\text{H}_2$  pressure of 0.33 atm.

Figure 3 shows the fraction of the carrier power converted into the frequency up-shifted sideband,  $P_{750}/P_{785}$ , as the incident pump power is varied and the  $\text{H}_2$  pressure is held

constant at 0.33 atm. The highest conversion efficiency that we achieve is  $2.3 \times 10^{-6}$ . The fraction of total power converted into both 750 nm and 823 nm is  $3 \times 10^{-6}$ . We observe efficiencies within a factor of two of Fig. 3 for gas pressures between 0.05 and 1.5 atm. For example, at a pressure of 0.08 atm, the modulation efficiency is only 30% lower than shown in Fig. 3. As discussed in Refs. [14, 25], the modulation process is coherent, and as a result, the carrier and the two sidebands have a well-defined, although initially unknown, relative phase. This phase can be detected and varied using a phase mask, and these three beams can be used to synthesize, for example, AM or FM waveforms.

One of the key advantages of our modulator is that it can be used to modulate any frequency within the optical region of the spectrum. This is because of the large transparency window of the  $\text{H}_2$  molecules and the low operating pressure.  $\text{H}_2$  molecules are not infrared-active, and the first electronic resonance occurs in the Lyman band at a wavelength of 111 nm. Figure 4 shows the predicted efficiency of our modulator to the frequency upshifted sideband over the wavelength range 120 nm to 10  $\mu\text{m}$  at gas pressures of 0.33 atm (solid line) and 0.08 atm (dashed line). Here, we use the matrix elements and energy levels of the ro-vibrational levels in the Lyman and Werner bands [27] and calculate the dispersion and Raman coupling of  $\text{H}_2$  at different wavelengths. We then use these results to numerically solve propagation equations that describe the generation of the sideband from the carrier [28]. We also include diffractive effects and estimate the mode overlap of the carrier with the pump and the Stokes beams in the cavity. Generally, as the wavelength of the carrier beam becomes shorter, an increase in the modulation efficiency is expected. This is due to three reasons: i) an increase in the Raman coupling since the frequencies get closer to the electronic resonances, ii) the propagation equations' linear scaling with frequency, and iii) better mode overlap of the carrier beam with the pump and the Stokes due to reduced divergence of the beam. This general trend is seen in Fig. 4. The figure also illustrates that this increase in efficiency with decreasing wavelength persists only up to a certain wavelength, after which the efficiency drops sharply. The drop is due to the sideband-carrier phase mismatch becoming a significant factor. Because there is lower dispersion at lower pressures, the peak efficiency at 0.08 atm happens at a shorter wavelength than at 0.33 atm. We note that Fig. 4 represents the maximum useable bandwidth of our modulator and does not take into account the transmissivity of the cavity mirrors nor of the vacuum chamber windows. In our experiment, the mirrors and windows are made from a fused silica substrate

which transmits well in the region 170 nm–3  $\mu\text{m}$ . If the modulator is used outside of this spectral region, a different substrate for the optics will need to be used, for example LiF for wavelengths shorter than 170 nm.

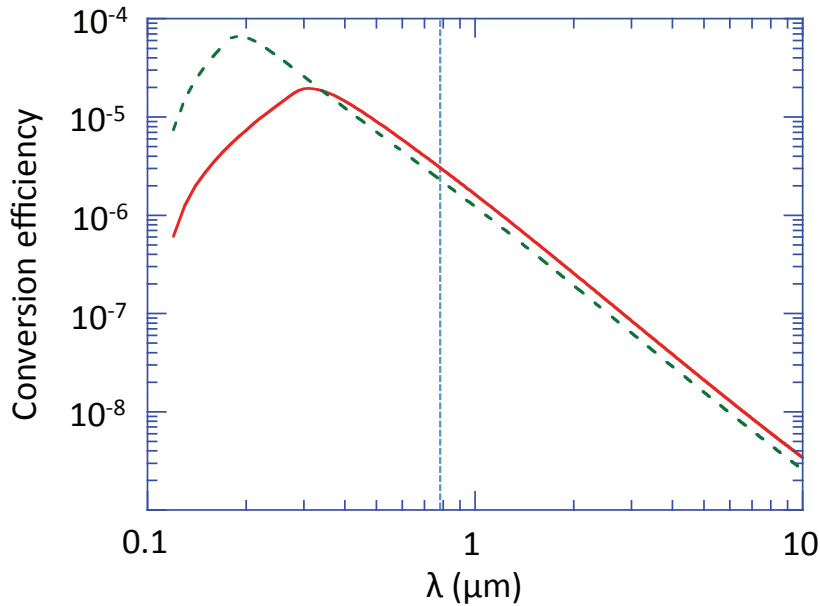


FIG. 4: Predicted conversion efficiency of our modulator as a function of the wavelength of the carrier for  $\text{H}_2$  pressures of 0.33 atm (solid line) and 0.08 atm (dashed line). The vertical dotted line marks 785 nm, which is the carrier wavelength used in our experiment. The conversion efficiency only increases with decreasing wavelength to a certain point, below which a phase-mismatch between the sideband and the carrier decreases the efficiency.

We next discuss several future directions of our work. The biggest limitation of our current experiment is the low modulation efficiency. Increasing the efficiency requires higher pump and Stokes intracavity intensities in order to establish higher molecular coherence. Currently, the pump and Stokes intensities are largely determined by the Raman lasing process, and they are not close to the damage threshold of the cavity mirrors. This limitation may be overcome using an independent laser beam locked to the cavity as the Stokes beam. We also note that although we have focused on modulating a monochromatic laser beam in this work, this device can also be used to modulate broadband signals. One intriguing application is to modulate a frequency-comb Ti:sapphire laser oscillator [29, 30]. A typical frequency-comb

has several hundred thousand teeth covering the spectral region 700 nm–900 nm. If such a broadband signal passes through a molecular modulator, each tooth produces frequency up-shifted and down-shifted sidebands, greatly extending the spectral coverage of the comb. For example, using the fundamental vibrational transition in H<sub>2</sub> ( $\nu_m = 124.6$  THz), the comb may be expanded to cover from 540 nm to 1.4  $\mu\text{m}$  after a single pass through the modulator.

We thank Nick Brewer, Daniel Sikes, and Zach Simmons for experimental assistance and many helpful discussions. This work was supported by the National Science Foundation (NSF) and University of Wisconsin-Madison.

- 
- [1] B. Boyd, *Nonlinear Optics* (Academic Press, San Diego).
  - [2] M. Chacinski *et al.*, *J. Lightwave Tech.* **27**, 3410 (2009).
  - [3] S. Yoshikawa and T. Imasaka, *Opt. Commun.* **96**, 94 (1993).
  - [4] A. E. Kaplan, *Phys. Rev. Lett.* **73**, 1243 (1994).
  - [5] Th. Udem, R. Holzwarth, and T. W. Hänsch, *Nature (London)* **416**, 233 (2002).
  - [6] M. M. Boyd *et al.*, *Science* **314**, 1430 (2006).
  - [7] H. S. Margolis *et al.*, *Science* **306**, 1355 (2004).
  - [8] T. W. Hänsch, *Rev. Mod. Phys.* **78**, 1297 (2006).
  - [9] J. L. Hall, *Rev. Mod. Phys.* **78**, 1279 (2006).
  - [10] R. S. Judson and H. Rabitz, *Phys. Rev. Lett.* **68**, 1500 (1992).
  - [11] T. Baumert, T. Brixner, V. Seyfried, M. Strehle, and G. Gerber, *Applied Physics B* **64**, 265 (1997).
  - [12] M. Shapiro and P. Brumer, *Rep. Prog. Phys.* **66**, 859 (2003).
  - [13] N. Zhavoronkov and G. Korn, *Phys. Rev. Lett.* **88**, 203901 (2002).
  - [14] A. V. Sokolov, D. D. Yavuz, D. R. Walker, G. Y. Yin, and S. E. Harris, *Phys. Rev. A* **63**, 051801(R) (2001).
  - [15] A. V. Sokolov, D. R. Walker, D. D. Yavuz, G. Y. Yin, and S. E. Harris, *Phys. Rev. Lett.* **85**, 562 (2000).
  - [16] J. Q. Liang, M. Katsuragawa, F. Le Kien, and K. Hakuta, *Phys. Rev. Lett.* **85**, 2474 (2000).
  - [17] T. Suzuki, M. Hirai, and M. Katsuragawa, *Phys. Rev. Lett.* **101**, 243602 (2008).

- [18] M. Y. Shverdin, D. R. Walker, D. D. Yavuz, G. Y. Yin, and S. E. Harris, *Phys. Rev. Lett.* **94**, 033904 (2005).
- [19] W. Chen *et al.*, *Phys. Rev. Lett.* **100**, 163906 (2008).
- [20] H. Chan *et al.*, *Science* **331**, 1165 (2011).
- [21] F. Couny, F. Benabid, and P. S. Light, *Phys. Rev. Lett.* **99**, 143903 (2007).
- [22] J. K. Brasseur, K. S. Repasky, and J. L. Carlsten, *Opt. Lett.* **23**, 367 (1998).
- [23] J. K. Brasseur, P. A. Roos, K. S. Repasky, and J. L. Carlsten, *J. Opt. Soc. Am. B* **16**, 1305 (1999).
- [24] S. Zaitsev, H. Izaki, and T. Imasaka, *Phys. Rev. Lett.* **100**, 073901 (2008).
- [25] J. T. Green, J. J. Weber, and D. D. Yavuz, *Phys. Rev. A* **82**, 011805(R) (2010).
- [26] J. T. Green, J. J. Weber, and D. D. Yavuz, *Opt. Lett.* **34**, 2563 (2009).
- [27] H. Abgrall and E. Roueff, *Astron. Astrophys. Suppl. Ser.* **79**, 313 (1989).
- [28] S. E. Harris, and A. V. Sokolov, *Phys. Rev. A* **55**, R4019 (1997).
- [29] F. Le Kien, S. N. Hong, and K. Hakuta, *Phys. Rev. A* **64**, 051803 (2001).
- [30] S. Gundry *et al.*, *Opt. Lett.* **30**, 180 (2005).